

Hot-Cold Spots in Italian Macroseismic Data

G. Molchan^{1,2}, T. Kronrod^{1,2}, G.F. Panza^{1,3}

¹⁾ *The Abdus Salam International Centre for Theoretical Physics, SAND group, Trieste, Italy*

²⁾ *International Institute of Earthquake Prediction Theory and Mathematical Geophysics, Russian Academy of Sciences, Moscow*

³⁾ *Department of Earth Sciences, University of Trieste, Italy*

Abstract. The site effect is usually associated with local geological conditions, which increase or decrease the level of shaking compared with standard attenuation relations. We made an attempt to see in the macroseismic data of Italy some other effects, namely, hot/cold spots in the terminology of Olsen (2000), which are related to local fault geometry rather than to soil conditions. We give a list of towns and villages liable to amplify (+) or to reduce (–) the level of shaking in comparison with the nearby settlements. Relief and soil conditions cannot always account for the anomalous sites. Further, there are sites where both (+) and (–) effects are observed depending on the earthquake. The opposite effects can be generated by events from the same seismotectonic zone and along the same direction to the site. Anomalous sites may group themselves into clusters of different scales. All isolated anomalous patterns presented in this paper can be used in hazard analysis, in particular, for the modeling and testing of seismic effects.

Key words: site effect, seismic intensity, macroseismic data, seismic hazard

I. Introduction. The impact of earthquake waves on a structure, referred to as *seismic input* below, is the combined effect of the earthquake rupture process, travel path, and site conditions. The uppermost – unconsolidated layers and the topography make significant contributions to the seismic input. It is a known fact (see, e.g., Mercalli, 1907; Bard & Bouchon, 1980; Shteinberg et al., 1993; Joyner, 2000; Field et al., 2000; Panza et al., 2001; Cornou et al., 2003) that the seismic input is enhanced in shallow valleys owing to the generation of high-amplitude local surface waves. This amplification in deep valleys is due to possible resonances. When the contrast between bedrock and sediment is high, the motion becomes much longer owing to multiple reflections of surface and body waves within the basin (e.g. Zuccolo et al., 2008). When the soil layer is unconsolidated and dipping, seismic rays may experience focusing. This latter effect for a plane seismic wave depends on the angle of emergence, hence is unstable.

Routinely the seismic input is ranked by peak acceleration or velocity in the frequency range 0 to 10 Hz. There are many simple recipes for assessing the seismic input, termed attenuation relations (for a review see Douglas, 2003). Significant deviations – by factors of two or more – of the observed seismic input from the value predicted by these relations are relegated to the category of site effect.

The attenuation relations usually apply to the average soil. For this reason a local departure from the model leads to a regular site effect and is corrected for local soil conditions. However, the origin of site effects is much more diversified, as follows from the above-mentioned facts. Moreover, the anomalous patterns can appear both at different scales and stochastically; one cause of this consists in earth structure complexity, hence the instability of the effect.

Field and SCEC Working Group (2000), Olsen (2000) published 3-D computer simulations of earth ground-motion amplification in southern California. They show that each earthquake exhibits unique “hotspots” of anomalous strong shaking, even when the local geological conditions are taken into account. Hotspots depend on specific details of the earthquake, such as orientation of the fault, irregularities of the rupturing fault surface, and wave scattering, which depends on subsurface structures.

It is natural that a realistic reproduction of this effect requires detailed earthquake and environment information. There are also limitations associated with computational techniques and with local instabilities in the seismic input. In this connection macroseismic data are of independent interest because they contain information on a wide range of seismic input over a large territory. Below we deal with Italian data that are available for a long time span (a few hundred years) and sample almost the entire region.

We remind the essential properties of the macroseismic measure of seismic input, i.e., intensity I :

- (a) it is not an instrumental quantity; nevertheless, the change in I by unity in the MSK- or MCS-type scales roughly corresponds to the change in peak acceleration by a factor of 2 to 2.5 (Cancani, 1904; Shteinberg et al., 1993; Panza et al., 1997; Shebalin & Aptikaev, 2003); therefore, the deviation ΔI of

- observed I from the expected value as large as $|\Delta I| \geq 1$ is here considered anomalous;
- (b) I is not a point characteristic; it is obviously statistical in character and records the average seismic input to an area of scale $L=1-10$ km (the size of a typical village);
- (c) I is a discrete quantity on an integer or half-integer scale. Non integer values are often reported to indicate the difficulty to assign the observed effect to a specific intensity degree.
- The properties (b) and (c) grant certain stability to I .

In the regular situation macroseismic intensity decays with distance, therefore, isoseismal areas of level I (the area with intensities of at least I) are embedded in isoseismal area of level $I-1$. A local anomaly of macroseismic intensity can disturb the simple connectivity of an isoseismal area and makes I to deviate from the expected value, i.e., produces *inversion* of I in the terminology of Shebalin (2003). The inversion of I may be positive or negative, isolated or clustered. We plan to analyze these features in Italian macroseismic data because they have to include the “hot/cold spots” patterns by Field & SCEC Working Group (2000).

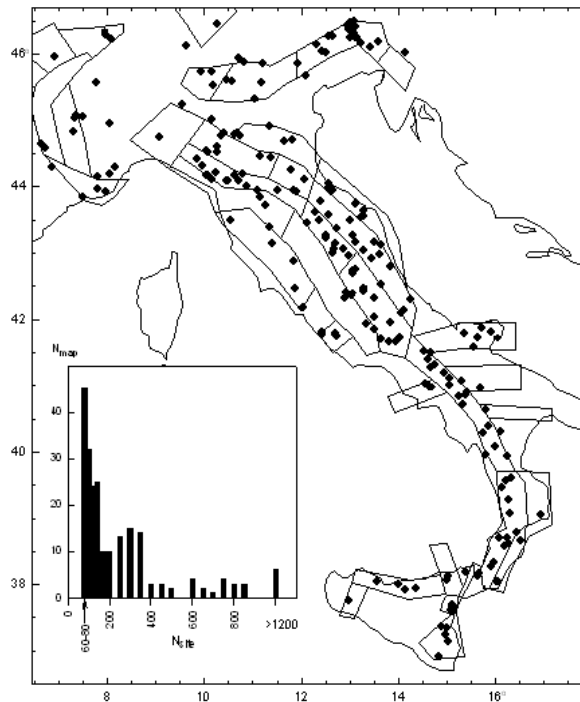


Fig. 1. Earthquakes selected for the analysis of I -maps. The inset shows the number of maps (N_{map}) with given number of sites (N_{site}). The *thin lines* show the seismic source zones by Miletti et al. (2008).

2. The Data. The CFTI catalog (Boschi et al., 2000) is used as the main source of Italian macroseismic data. This has been supplemented by data taken from the DOM database (Monachesi and Stucchi, 1997), Bolletino Macrosismico (BM, 1988-1993), and from the new DBMI04 database (2004).

For the purposes of this work we selected 229 I -maps, $I(g)$, using the following criteria:

- the number of observation sites in a map should be $N_1 \geq 60$;
- the map should contain observations of at least three integer-value levels;
- the observation sites should cover an area of linear extent $L > 100$ km.

As a result a typical I -map contains from 60 to 300 sites. For most of the selected events isoseismal maps have been produced in our previous publications (Kronrod et al., 1999, 2002).

To relate the data to the seismotectonic zones we use the Italian seismic source zone model by Meletti et al. (2008).

Figure 1 shows that the epicenters of the selected events provide a fairly good coverage of the seismogenic areas of Italy.

3. Empirical Analysis. With the exclusion of the regular site effect, Olsen (2000) in his 3-D computer simulations reproduce anomalous strong shaking patterns with the following properties: they are non-regular, isolated, and are ≤ 30 km in extent. Similarly, we would like to find such effects in macroseismic data. With this aim, primarily we identify the sites where isolated local I -inversions have been observed in the past. Next, for each selected site we classify the I -maps that contain this site.

First step. Choosing an $I(g)$ map, we classify a site g_0 on $I(g)$ as anomalous if

- 1) g_0 is outside the first isoseismal;
- 2) $I(g_0) \geq IV$;
- 3) g_0 has a sufficiently dense surrounding of nearby sites g_k relative to which $I(g_0)$ is an isolated local anomaly, i.e., as a rule, the deviation of I is large and has a uniform sign.

More exactly, the last requirement means that:

- 3a) the number of nearby sites $\{g_k\}$ is at least N_- , i.e., $N(g_0) \geq N_-$; in the following we take $N_- = 5$;
- 3b) the nearby sites are enclosed within a ring: $2 < |g_0 - g_k| < R$, where $R \leq 40$ km;
- 3c) all angles, α_k , between adjacent vectors $g_0 g_k$ are less than α_- .

To choice of α_- , note that

$$360^\circ = \sum \alpha_k \leq \alpha_- \cdot N(g_0),$$

therefore we can determine $\alpha_- = 72^\circ$ because $N(g_0) \geq 5$;

- 3d) at least $N(g_0) - 2$ nearby sites have identical values of

$$s(g) = \text{sign}(I(g_0) - I(g)),$$

say $s(g_k) = s$. All sites with $s(g) \neq s$ are considered to be "noise".

We admit the equality $I(g_k) = I(g_0)$ at one site at the most and the inequality

$$|I(g_0) - I(g_k)| < 1. \quad (1)$$

for 10% of the sites, at the most.

Thus, a g_0 site on an I -map acquires the sign $s(g_0|I) = s$ with values (+) or (-). If all requirements (1–3) are fulfilled with the exception of (3d) for any $R \leq 40$ km, then to the quantity $s(g_0|I)$ the value 0 (normal) is assigned. In the other cases $s(g_0|I)$ is treated as indeterminate.

Finally, the isolated site effect on an I -map is characterized by an anomalous deviation of $I(g_0)$:

$$s(g_0|I) \min'_k |I(g_0) - I(g_k)| = \Delta I(g_0). \quad (2)$$

Here the minimum is taken over all sites g_k with the exception of the "noise" sites in (d) and the sites which satisfy (1).

Examples of (+) and (-) sites are given in Fig. 2.

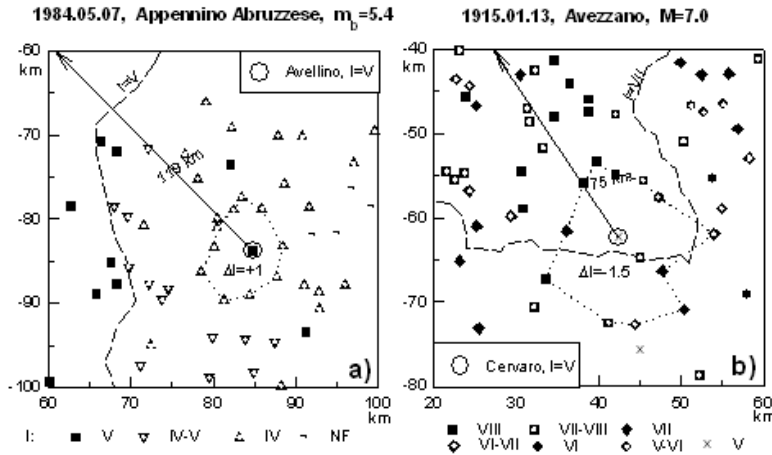


Fig. 2. Examples of isolated local anomalous sites:

(a) hot, (b) cold.

The *dashed line* indicates an isoseismal of level I ; the *dotted line* delimits the neighborhood of an anomalous site. The epicenter is used as the zero point in the Cartesian coordinates (in km). Notation $75 \downarrow$ means direction and distance in km to an epicenter.

Second step. For each selected anomalous site g_0 we revise all I -maps again and choose the maps that satisfy conditions 1 and 3 at g_0 . In other words, the requirement $I(g_0) \geq 4$ is omitted to increase the number of maps covering g_0 . As a result we have at g_0

$$\max_i I(g_0) \geq IV \geq \min_i I(g_0), \quad (3)$$

where the extremes are taken from the maps with $s(g_0|I) \neq 0$.

The subsequent discussion is limited to the sites for which

- 4) $N_{\text{map}}(g_0) \geq 7$, where N_{map} is the number of maps for which $s(g_0|I)$ have been assigned.

Now each anomalous site g_0 can be characterized by the following quantity:

$$f(g_0) = N_{\text{map}}(g_0) / N_a(g_0), \quad (4)$$

where $N_a(g_0)$ is the number of maps with $s(g_0|I) \neq 0$. The quantity $f(g_0)$ means that the local I -effect at g_0 is observed on average in each $f(g_0)$ -th map for which $s(g_0|I)$ have been assigned.

The anomalous sites are divided into three categories:

- ◆ those with a persistent nonnegative effect ("hot", +):

$$s(g_0|I) \geq 0 \text{ for any } I\text{-map} \quad (5)$$

- ◆ those with a persistent nonpositive effect ("cold", -):

$$s(g_0|I) \leq 0 \text{ for any } I\text{-map}; \quad (6)$$

- ◆ those with a mixed effect (hot/cold or +/-), i.e. there exist both maps with $s(g_0)=+$ and maps with $s(g_0)=-$.

Histograms of $f(g)$ for the three categories of sites are given in Fig. 3. They show that the typical range of $f(g)$ is (4, 10), i.e., typically the hot or cold effect is not a permanent feature of the anomalous site. The same property holds for the "hotspot" effect by Field and SCEC Working Group (2000). But our definition of an isolated local anomalous site is based on local features in the set of I -maps that cover the site, and thus is independent of any attenuation relation.

The three categories contain very different numbers of anomalous sites:

$$\#(+)=65; \quad \#(-)=21; \quad \#(+/-)=10. \quad (7)$$

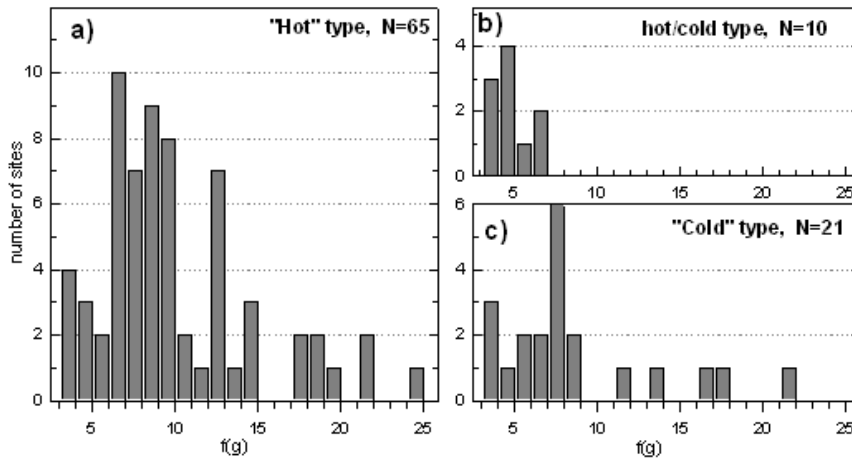


Fig. 3. Histograms of $f(g) = N_{\text{map}}/N_a$ for three types of sites: (a) hot (+), (b) mixed (+/-), and (c) cold (-).

The cause of this is twofold; on the one hand the type (-) sites were of less interest at the time the macroseismic effects were recorded, hence are less complete; on the other hand, our analysis of isolated local anomalies is asymmetrical with respect to the (+) and (-) types. The first step of analysis is concerned with the sites having $I(g_0) \geq IV$. When $I(g_0)=IV$, a vicinity of g_0 must contain sites with $I(g) \leq III$ if it is a (+) effect and with $I(g) \geq V$ if it is a (-) effect. These requirements are not equivalent and restrict the set of (-) sites.

Figure 4 and Table 1 summarize the anomalous sites that have been identified. They provide the spatial distribution of the sites, the characteristic $f(g_0)$, all events that have given rise to the anomaly at a site, the magnitude of the anomaly $\Delta I(g_0)$, and the epicenter-site distance. It is possible to conclude that an isolated anomalous site in Table 1 has the following typical properties:

- it is located 50-150 km from the epicenter;
 - the radius R of the neighborhood with respect to which g_0 is anomalous is 10-40 km (the upper bound, 40 km, is a consequence of condition 3b);
 - the number of sites around g_0 is 10-20;
 - the number of $I(g)$ maps that cover g_0 is 7-20 (the lower bound, 7, is a consequence of condition 4).
- Overall, the (+) and (-) sites cover the region uniformly enough, with the exception of the western Alps where the density of observation is low.

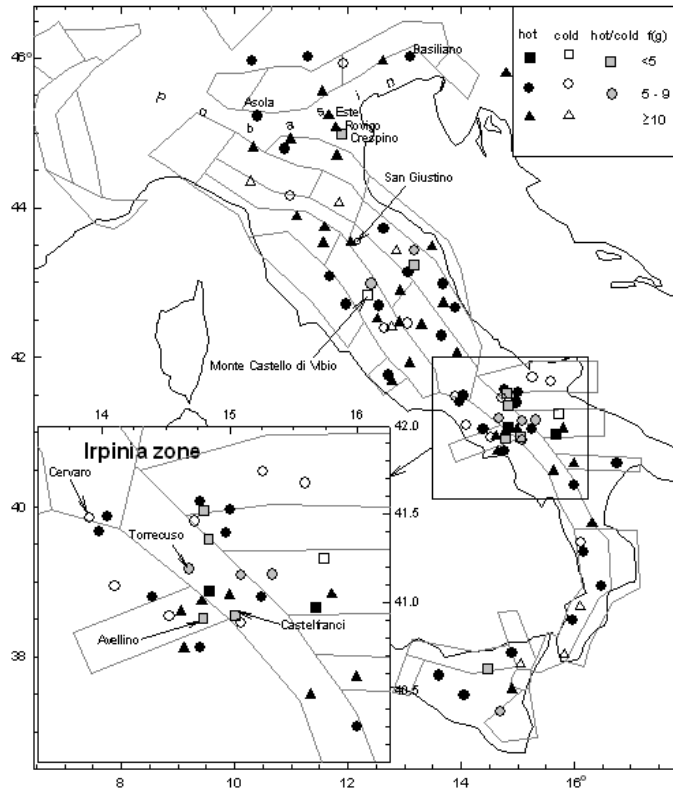


Fig. 4. Anomalous sites of three types (hot, cold, hot/cold) and their characteristic $f(g)$; the *thin lines* show the seismic source zones by Meletti et al. (2008).

4. Individual examples

4.1. Isolated local anomalies. In most cases the explanation of local anomalous effects is not obvious and not unique. For example, hot and cold effects would be naturally expected where an appreciable soil contrast exists between the site itself and its environs. A few sites in Fig. 4 fulfill these expectations. One of the more positive examples is the Monte Castello di Vibio site of type (-) (see Fig. 4). This site is on hard rock, while sediments cover the environs. The relationship is just the reverse for Avellino and its environs (Fig. 4). For this reason the hot effect is typical there (see Fig. 5a). However, the Gargano earthquake of August 12, 1889 (N 1 on Fig. 5a) produced $I = \text{II-III}$ at Avellino and $I = \text{IV}$ & $\underline{I} = \text{IV-V}$ for the environs, i.e., the cold effect, contrary to expectation. In principle, a case of this type is possible due to the influence of previous earthquakes on the vulnerability of structures (Baratta, 1906). But it is unlikely for the isolated effect.

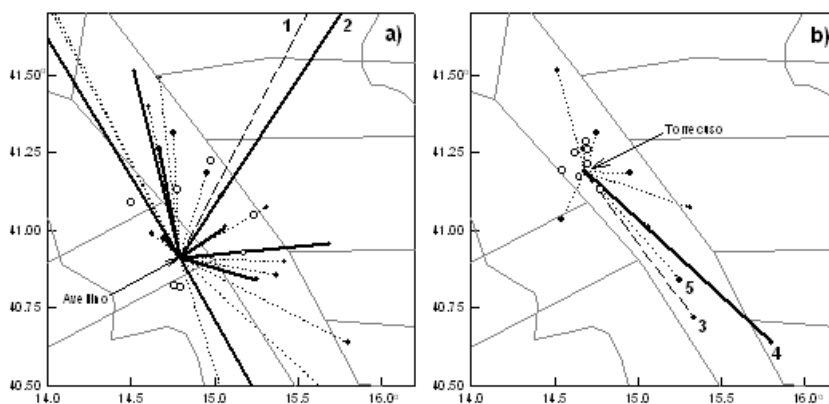


Fig. 5. Sites with (+/-) type effect: (a) Avellino and (b) Torreouso.

The lines (*bold, dotted or dashed*) connect the sites with events and indicate the type of local effect ((+), 0 or (-) respectively); *open circles* represent I -data points from the site neighborhood, which are encountered in all I -maps where the site is anomalous. Additional information on the events with numbers assigned in the plot: 1) 1889.12.08, Apricena, dist=120 km, $I(g_0)=2.5$, the local effect $\Delta I=-1$; 2) 1951.01.16, Gargano, dist=125 km, $I(g_0)=3.5$, $\Delta I=+0.5$ (doubtful (+)-effect); 3) 1990.05.05, Potenza, dist=83 km, $I(g_0)=\text{no felt}$, $\Delta I=-3$; 4) 1991.06.26, Potentino, dist=121 km, $I(g_0)=5$, $\Delta I=+1$; 5) 1980.11.23, Irpinia-Lucania, dist=53 km, $I(g_0)=6$, $\Delta I=0$.

The sites of (+/-) type are the most interesting for interpretation because the traditional explanation in terms of soil conditions and the thickness of sediment above hard bedrock is insufficient. Fig. 5b (see also Fig. 4) represents the Torrecuso site. Here three events have produced different effects at the site, namely (+), (-), and "normal" (0); at the same time they have similar directions toward the site.

In the deep sediment-filled Po Basin (see Fig. 4), the expected effect relative to the normal soil ought to be of type (+). This is confirmed by many events (see at least ten I -maps in Kronrod et al., 1999) occurring in the surrounding area because their isoseismals anomalously extend into the sediment zone. We are however interested in the isolated local I -effects observed in the Po Basin (see Fig. 4). In this particular case the site and its environs are in "identical" soil conditions, hence the type of the anomalous site is not clear beforehand. Fig. 4 shows four sites of type (+) and one site of type (+/-) in the Po Basin, i.e., isolated local anomalous sites are available here.

2. *Clustered anomalous effects*. Intensity inversion can also occur at large scales, some tens or hundreds of kilometers. In that case we should call the phenomenon a *collective or clustered anomalous effect*. Such effects can not be easily formalized. Therefore we will consider a few examples, which may be of interest for the simulation and testing of Earth models.

Fig. 6 represents two I -maps with a collective anomalous effect in the Po Basin. In the case of the 1898, Calestano, $M=4.7$ event (Fig. 6a), the isoseismal of level $I=III$ is overextended into the sediment zone (domain **A**). To interpret this pattern, we use a recent paper by Carletti and Gasperini (2003), who suggest a nonhomogeneous I -attenuation model for the entire territory of Italy. Namely, the increment of I between an epicenter (g_0) and a receiver (site g) is given by the following empirical relation

$$I(g_0)-I(g)=\varphi(|g_0-g|) + \int_0^{s_0} b_1(g_0 + s(g - g_0))ds + \int_{s_0}^1 b_2(g_0 + s(g - g_0))ds \quad (8)$$

where $s_0=\min(1, d/|g_0-g|)$ and $d=45$ km; the first part of (8), $\varphi(|\Delta g|)$, is an average isotropic attenuation relation for Italy while $b_i(g)$, $i=1, 2$ are responsible for the spatial variations of the relation in near (the case b_1) and far (the case b_2) zones relative to g_0 . In particular, a point g with $b_2(g)<0$ is a point of low attenuation of I with respect to the average model in the zone: $|g-g_0|>d$. The functions b_1 and b_2 are computed on meshes of 50 and 25 km.

Fig. 6 shows two isolines of $b_2(g)$ in the subarea of the Po Basin where $b_2(g)<0$ ($|b_2(g)|$ increases toward northeast). In the case of the Calestano event (Fig. 6a) the model (8) well explains the anomalous part of the $I=III$ zone (domain **A**), namely, the shape and level of that zone.

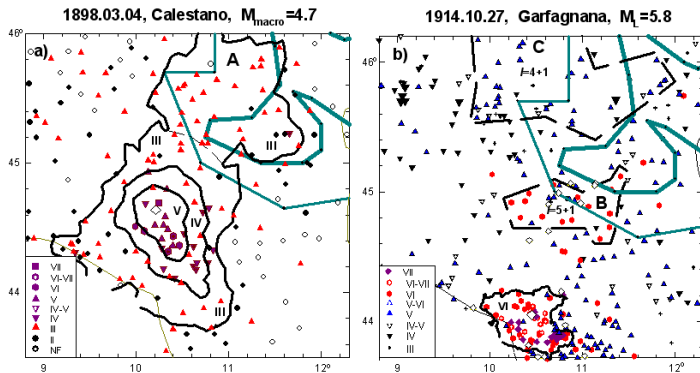


Fig. 6. Examples of clustered anomalous patterns in the Po Basin for the following events: (a) 1898, Calestano, $M=4.7$, and (b) 1914, Garfagnana, $M=5.8$.

Isoseismals (*bold line*) are based on the Modified Polynomial Filtering (MPF) method by Molchan et al. (2004); domain **A** is an anomalous part of the $I=III$ zone for the Calestano event, a natural boundary of the $I=III$ zone is given by a *dashed thin line*; domains **B** and **C** are zones of collective I -inversion for the Garfagnana event. The *open diamond* marks the epicenter.

Gray line is the level of low-attenuation of I according to Carletti & Gasperini (2003) (see main text).

The I -map for the 1914, Garfagnana earthquake, $M=5.8$ (Fig. 6b) has anomalous features practically in the same place. The isoseismal zone of level $I=VI$ consists of two parts, the main and the isolated anomalous zone **B** of type (+). There is also zone **C**, which looks as an anomalous isolated $I=IV$ zone of the same type (+). Therefore the pattern $\mathbf{B} \cup \mathbf{C}$ can be interpreted as a result of the expansion of the highest seismic intensities into the sediment zone of the Po Basin. As Fig. 6b shows, the model (8) is in agreement with the pattern $\mathbf{B} \cup \mathbf{C}$ but only qualitatively. This model can not explain both the disconnection of the isoseismal zone $\{I \geq VI\}$ and the I -level of the pattern **C**

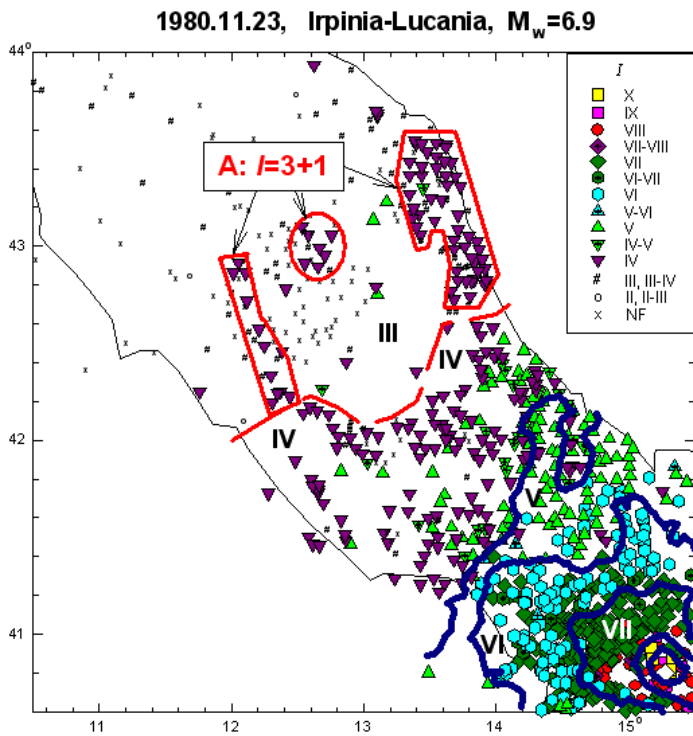


Fig. 7. I -map (northern part) for the 1980, Irpinia-Lucania, $M=6.9$ earthquake. Isoseismals (blue lines) are based on the MPF method by Molchan et al. (2004). Domain **A** (bold red lines) is an anomalous part of $I=IV$ zone; a natural boundary of $I=IV$ zone is given by dashed red line. The open diamond marks the epicenter.

An interesting example with an overextended I zone is provided by the I -map of 1980, Irpinia-Lucania, $M=6.9$ event (Fig. 7). The anomalous part of the $I=IV$ zone consists of three disconnected pieces (see zone **A**) and lies in the far zone relative to the epicenter. The model (8) is non-informative at all in this case. The pattern **A** is unique for the Umbria-Marche domain (see the Atlas by Kronrod et al., 2002) and therefore it is interesting for interpretation.

The next two examples (Fig. 8, Fig. 9) illustrate an isolated collective anomalous effect of size 30-50 km. The first one is the I -map of the 1987, Porto San Giorgio earthquake (Fig. 8). Here, the $\{I \geq V\}$ -zone has a well-pronounced anomalous part **B** of size $L=45$ km; **B** is within the $I=III$ isoseismal. The anomaly is situated in the northern Umbria-Marche Apennines and is adjacent to the transition zone that separates the central and the northern Apennines. The sites showing the (+) effect ($\Delta I = 2$) are situated at different altitudes, between 270 m and 430 m (ref. GG), and on different soils, ranging from limestone and shale to Quaternary alluvium. Model (8) is again unable to explain the isolated effect. In addition, it cannot explain the strong effect ($\Delta I = +2$) in **B**.

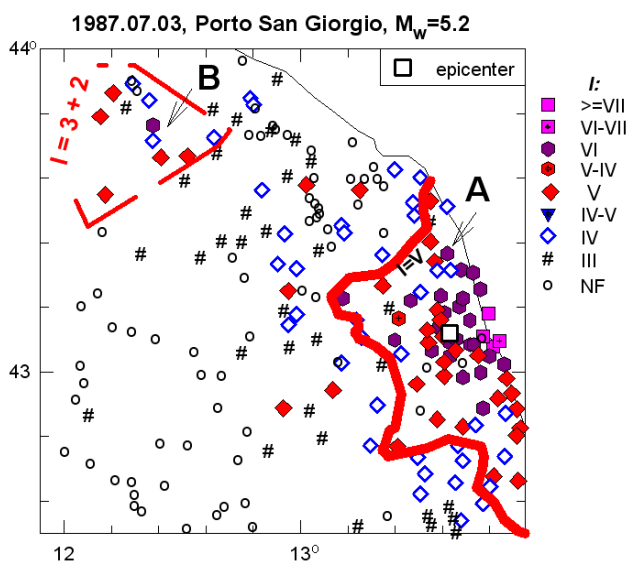


Fig. 8. Example of isolated anomalous patterns of type (+): I -map of 1987, Porto San Giorgio, $M=5.2$ earthquake. The $\{I \geq V\}$ zone consists of two parts: main (**A**) and anomalous pattern (**B**); the effect in **B** is $\Delta I = +2$.

The I -map of the 1984, Apennino Abruzzese, $M=5.9$, earthquake is another example of the isolated collective anomalous effect but now of type (-) (see Fig.9). This effect is localized in a wedge-like zone between the W-E Circeo-Vulture line and the NNW-SSE Appenine fault system. The sites within **C** are situated at different altitudes, between 297 m and 981 m (ref. GG), on slopes with different steepness, and in different soil conditions ranging from volcanic bedrock to young sedimentary deposits (CNR P.F. Geodinamica, 1992).

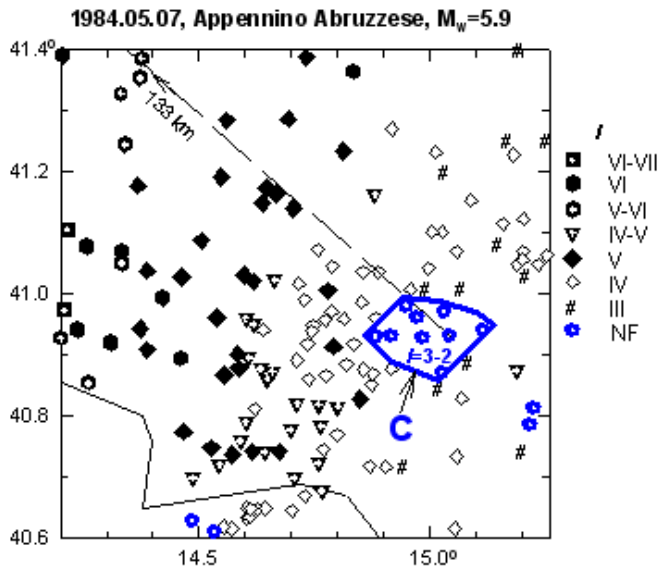


Fig. 9. Example of isolated collective anomaly of type (-): I -map of the 1984, Apennino Abruzzese, $M=5.9$ earthquake; **C** is anomalous zone of type (-); the effect in **C** is $\Delta I=-2$; $\uparrow 133$ km indicates direction and distance from zone **C** to the epicenter.

To understand the effect in **C** we considered twenty I -maps that cover **C**. The epicenters of the events concerned are plotted in Fig. 10. All events to the north of the Circeo-Vulture fault system have only the non-positive effect in **C**. To be specific, 3 events out of 8 produce normal effect and 5 produce a cold spot. The other 12 events produce normal effect in **C** and occur either on the Circeo-Vulture faults or to the south of **C**. Thus, we may suppose that the cause of the (-) effect in **C** is the strong attenuation of the seismic waves travelling across the Circeo-Vulture fault system from north to south. In the framework of model (8) we should expect the (+) effect at those sites of **C** where (-) has been observed. Indeed, let us connect each event which generates a (-) effect in **C** with **C** by a segment (see Fig. 10). On the figure we can see the trace of the intersection of the segment with the low I -attenuation zone according to (8); since the trace dominates in each segment, we have a (+) effect in **C**.

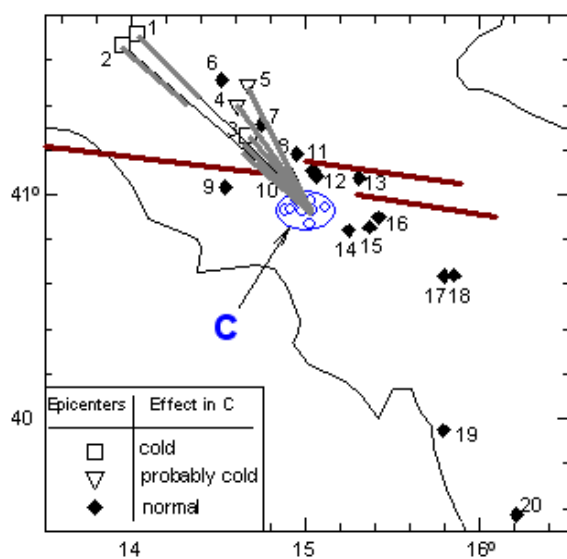


Fig. 10. The anomalous zone **C** (oval) shown in Fig. 9 and 20 events whose I -maps cover **C**:

- 1) 1984.05.07, $M=5.9$; 2) 1984.05.11, $M=5.5$;
- 3) 1688.06.05, $M=6.6$; 4) 1456.12.05, $M=7.1$; 5) 1913.10.04, $M=5.2$;
- 6) 1805.07.26, $M=6.7$; 7) 1997.03.19, $M=4.6$;
- 8) 1962.08.21, $M=6.2$; 9) 1903.05.04, $M=5.0$;
- 10) 1905.03.14, $M=4.7$; 11) 1905.11.26, $M=5.1$;
- 12) 1732.11.29, $M=6.4$; 13) 1930.07.23, $M=6.7$;
- 14) 1980.11.23, $M=6.9$; 15) 1694.09.08, $M=7.0$;
- 16) 1910.06.07, $M=5.9$; 17) 1991.05.26, $M=4.7$;
- 18) 1990.05.05, $M=5.8$;
- 19) 1982.03.21, $M=5.0$;
- 20) 1887.12.03, $M=6.4$.

C consists of sites (blue open circles). Each event, which generates a (-) effect in **C**, is connected with **C** by segment.

A trace of the low I -attenuation zone by Carletti & Gasperini (2003) on the segment is marked by gray color.

Bold brown lines show the Circeo-Vulture fault system

5. Conclusion. The *site effect* is usually associated with local geological conditions, which increase or decrease the level of shaking in comparison with standard attenuation relations. We made an attempt to evidence in macroseismic data some other effects namely *hot/cold spots* in the terminology of Olsen (2000), which is related to local fault geometry rather than to soil conditions. Our analogue of this effect (*isolated I-inversion*) is based on local features in the set of *I*-maps that cover a site, and thus is independent of the reference attenuation model.

The local *I*-inversions are not persistent. They are not very frequent (roughly in 10-25% of the considered cases where abnormal intensities are identified); the relative effect (ΔI) may be either +1 or -1 for different earthquakes. It thus appears that the topography and soil conditions are necessary, but far from sufficient for an interpretation of the *I*-inversions. Thus, our collection of *I*-inversions (Table 1) includes the hot/cold effects as defined by Olsen (2000).

Engineering studies of site effects are relevant to the near zone and $I \geq VIII$ (Shteinberg et al., 1993). Our examples exclude the first isoseismal (the near zone) and are limited to the range $I < X$ (MCS) and distances not exceeding 200 km, consequently they serve as a complement to engineering experience.

Intensity inversion can occur at large scales, some tens or hundreds of kilometres as well. The non-homogeneous attenuation model by Carletti & Gasperini (2003) could be useful in the interpretation of such patterns, however, the examples show that this model is far from being always applicable. Therefore, all our *I*-inversion patterns (see Table 1, Figures 5–9) are of interest for the simulation and testing of the seismic input. The list of anomalous sites given in Table 1 is incomplete because of the stringent selection criteria used and the classification of the sites as hot, cold or hot/cold may be modified as more data become available.

Acknowledgements. We are grateful to the anonymous reviewers for the careful reading of the paper and very useful comments and suggestions. This work was supported by the Russian Foundation for Basic Research through grant 08-05-00215, and by the ASI-Pilot project SISMA

References

- Baratta M. (1906) Il grande terremoto Calabro dell'8 settembre 1905. Alcune considerazioni sulla distribuzione topografica dei Danni. Atti Soc. Toscana Sc. Natur., v. XVI, N 1, 13-18.
- Bard P., Bouchon M. (1980) The seismic response of sediment-filled valleys. 1. The case of incident SH-waves. Bull. Seismol. Soc. Amer., v. 70, N 1, 1263–1286.
- BM: Bolletino Macrosismico, 1988-1993. Istituto di Geofisica, Unita Operativa Geodinamica, Roma
- Boschi E., Guidoboni E., Ferrari G., Margotti D., Valensise G. and Gasperini P. (2000) Catalogue of strong Italian earthquakes from 461 B.C. to 1997. Introductory texts and CD-ROM. Annali di Geofisica, v. 43, N 4, 609-868.
- Cancani A. (1904) Sur l'emploi d'une double echelle seismique des intensites, empirique et absolue, G. Beitr, Vol. 2, pp. 281-283.
- Carletti F. and Gasperini P. (2003) Lateral variations of seismic intensity attenuation in Italy. Geophys. J. Int., v. 155, 839-856.
- CNR. P.F. Geodinamica (1992) Structural model of Italy 1:500,000. S.EL.CA., Florence, Italy.
- Cornou C., Bard P., and Dietrich M. (2003) Contribution of dense array analysis to the identification and quantification of basin-edge induced waves. Part 2. Application to Grenoble basin (French Alps). Bull. Seismol. Soc. Amer., v. 93, N 6, 2624–2648.
- DBMI04: Database macrosismico Italiano (2004), INGV, <http://emidius.mi.ingv.it>
- Douglas J. (2003) Earthquake ground motion estimation using strong-motion records: a review of equations for the estimation of peak ground acceleration and response spectral ordinates. Earth Science Review, v. 6, 43-104.
- Field E.H. and SCEC Phase III Working Group (2000) Accounting for site effects in probabilistic seismic hazard analyses of Southern California: overview of the SCEC Phase III report. Bull. Seism. Soc. Am., v. 90, N 6B, S1–S31.
- GG: Global Gazetteer. Version 2.1. www.fallingrain.com/world/IT
- Joyner W.B. (2000) Strong motion from surface waves in deep sedimentary basins. Bull. Seism. Soc. Am., v. 90, N 6B, S95–S112.
- Kronrod T.L., Molchan G.M., Panza G.F. (1999) Atlas of isoseismal maps for Italian earthquakes 1400–1997, IC/IR/99/15, Internal report, ICTP, Trieste, 193 pp.
- Kronrod T.L., Molchan G.M., Podgaetskaya, V.M., Panza G.F. (2002) Formalized Representation of Isoseismal Uncertainty for Italian Earthquakes. Bolletino di Geofisica Teorica ed Applicata. Vol. 41, No. 3-4, 243-313.
- Meletti C., Galadini, F., Valensise, G., Stucchi, M., Basili, R., Barba, S., Vannucci, G., Boschi, E. (2008) A seismic source zone model for the seismic hazard assessment of the Italian territory. Tectonophysics, v.420, 85-108. http://zonesismiche.mi.ingv.it/elaborazioni/dati_di_ingresso
- Mercalli G. (1907) Sur le tremblement de terre calabrias du 8 septembre 1905. Comp. Rend. Acad. Sc., Paris, v. 144, 111-113.

- Molchan, G.M., Kronrod T.L., Panza G.F. (2004) The shape of empirical and synthetic isoseismals: comparison for Italian M<6 earthquakes. Pure and Appl. Geophys, 161, 1-23.
- Monachesi G. and Stucchi M. (1997) DOM 4.1, an intensity data base of damaging earthquakes in the Italian area. GNDT, at <http://emidius.itim.mi.cnr.it/DOM/home.html>.
- Olsen K.B. (2000) Site amplification in the Los Angeles basin from three-dimensional modeling of ground motion. Bull. Seism. Soc. Am., 90, 6B, p. 577-594.
- Panza G.F., Cazzaro R., Vaccari F. (1997) Correlation between macroseismic intensities and seismic ground motion parameters. Annali di Geofisica, Vol. XL. N 5. 1371–1382.
- Panza G.F., Romanelli F., Vaccari F. (2001) Seismic wave propagation in laterally heterogeneous anelastic media: theory and applications to seismic zonation. Advances in Geophysics, v. 3
- Shebalin N.V. (2003) Quantitative macroseismics. In: Computational seismology, Issue 34, Moscow. P. 57-200 (in Russian).
- Shebalin N.V., Aptikaev F.A. (2003) Development of MSK scales. Computational Seismology, Issue 34, p. 210-254 (in Russian).
- Shteinberg V., Saks M., Aptikaev F., Alkaz V., Gusev A., Erokhin L., Zagradnik I., Kendzera A., Kogan L., Lutikov A., Popova E., Rautian T., Chernov Yu. (1993). Methods of seismic ground motions estimation (Handbook). Seismic ground motions prediction (Engineering seismology problems; Issue 34), Moscow, Nauka, 5-94. (in Russian)
- Zuccolo, E., Vaccari, F., Peresan, A., Dusi, A., Martelli, A., Panza, G. F., (2008). Neo-deterministic definition of seismic input for residential seismically isolated buildings. Engineering Geology, v. 101, 89-95.

Table 1. Anomalous sites and their characteristics

#	Site g_0 (province)	coordinates		type $s(g_0)$	$f(g)=$ N_{map}/N_a	I -map [*]				
		Lat	Long			EQ date	I_0	dist	$I(g_0)$	$\Delta I(g_0)$
1	Accadia (FG)	41.158	15.334	+/-	14/2	1990.05.05	7	49	4.5	+1
						1984.05.07	8	137	5	-1
2	Acquasparta (TR)	42.690	12.546	+	10/2	1984.05.11	7	175	4	+1
						1984.04.29	7	65	5	+1
3	Altavilla Irpina (AV)	41.006	14.779	+	10/1	1984.05.07	8	110	5	+1
4	Anghiari (AR)	43.540	12.054	+	13/1	1920.09.07	9.5	173	5	+1
5	Ariano Irpino (AV)	41.153	15.089	+	18/1	1456.12.05	11	52	9.5	+1
6	Asola (MN)	45.221	10.413	+	10/2	1920.09.07	9.5	112	5.5	+1
						1987.05.02	6	55	5	+1
7	Asolo (TV)	45.801	14.791	+	12/1	1987.05.02	6	137	4	+1
8	Avellino (AV)	40.914	14.791	+/-	24/6	1732.11.29	9.5	24	9	+1
						1805.07.26	10	74	8	+1
						1889.12.08	7	120	2.5	-1
						1980.11.23	9.5	40	8	+1
						1982.03.21	7.5	149	5	+1
1984.05.07	8	119	5	+1						
9	Bagaladi (RC)	38.026	15.821	-	12/1	1783.03.28	10	93	5	-1
10	Baiano (AV)	40.951	14.618	+	11/1	1910.06.07	9	68	7	+1.5
11	Baronissi (SA)	40.746	14.770	+	9/1	1910.06.07	9	54	7	+1
12	Baselice (BN)	41.393	14.973	+	9/1	1991.05.26	7	118	4.5	+1
13	Basiliano (UD)	46.013	13.109	+	8/1	1988.02.01	6	27	5.5	+1
14	Breno (BS)	45.956	10.303	+	9/1	1936.10.18	9	161	6	+1
15	Brienza (PZ)	40.478	15.628	+	10/1	1905.09.08	11	210	6	+1
16	Caltanissetta (GL)	37.490	14.057	+	8/1	1990.12.13	7.5	89	5.5	+1
17	Camerino (MC)	43.135	13.068	+	28/3	1980.11.23	9.5	338	5	+1
						1984.05.07	8	190	4	+1
						1984.05.11	7	189	4	+1
18	Campoli (TE)	42.726	13.686	+	13/1	1984.05.07	8	124	5	+1
19	Cantalice (RI)	42.466	12.904	+	13/1	1987.07.03	7	87	4	+1
20	Capizzi (ME)	37.848	14.479	+/-	9/2	1905.09.08	11	157	6	+1
						1908.12.28	11	104	4	-1
21	Carpi (MO)	44.784	10.885	+	17/2	1919.06.29	9	111	6	+2
						1920.09.07	9.5	77	6	+1
22	Cassano allo Ionio (CS)	39.784	16.317	+	10/1	1980.11.23	9.5	162	6	+1

#	Site g_0 (province)	coordinates		type $s(g_0)$	$f(g)=$ N_{map}/N_a	I -map [*]				
		Lat	Long			EQ date	I_0	dist	$I(g_0)$	$\Delta I(g_0)$
23	Castel Giorgio (TR)	42.708	11.979	+	7/1	1993.06.05	6	69	5	+1.5
24	Castelfranci (AV)	40.931	15.043	+/-	8/2	1990.05.05 1991.05.26	7.0 6.5	37 76	6.5 1	+1.5 -2
25	Cercemaggiore (CB)	41.460	14.722	-	9/1	1688.06.05	11	21	6	-1
26	Cervaro (FR)	41.481	13.904	-	8/1	1915.01.13	11	75	5	-1.5
27	Collagna (RE)	44.347	10.275	-	18/1	1920.09.07	9.5	15	7	-1
28	Colle Sannita (BN)	41.361	14.833	+	13/2	1984.05.07 1984.05.11	8 7	86 83	6 6	+1 +1
29	Concordia sulla Secchia (MO)	44.914	10.981	+	10/2	1891.06.07 1971.07.15	9 7.5	72 46	6 7	+1 +1
30	Contigliano (RI)	42.411	12.769	-	14/1	1979.09.19	8	39	4.5	-1
31	Cossignano (AP)	42.983	13.688	+	7/1	1915.01.13	11	104	7.5	+1
32	Crespino (RO)	44.982	11.885	+	7/1	1987.05.02	6	93	5	+1
33	Deruta (PG)	42.982	12.420	+/-	14/2	1930.10.30 1998.03.26	8.5 6.5	93 57	5 4	+1 -1
34	Este (PD)	45.228	11.656	+	15/1	1914.10.27	7	134	6	+1
35	Ginosa (TA)	40.578	16.758	+	7/1	1905.09.08	11	209	6	+1
36	Grazzanise (CE)	41.091	14.102	-	8/1	1984.05.07	8	68	5	-1
37	Jelsi (CB)	41.518	14.796	+/-	8/2	1915.01.13 1980.11.23	11 9.5	129 90	6.5 4	+1.5 -1
38	Lavello (PZ)	41.046	15.795	+	10/1	1857.12.16	10.5	75	4	+1
39	Lercara Friddi (PA)	37.748	13.603	+	7/1	1908.12.28	11	180	7	+1
40	Levico Terme (TN)	46.011	11.303	+	8/1	1976.12.13	7	38	6	+1
41	Marcianise (CE)	41.033	14.395	+	7/1	1915.01.13	11	139	7	+1
42	Micigliano (RI)	42.451	13.054	-	9/1	1915.01.13	11	63	5	-1
43	Miglierina (CZ)	38.947	16.471	+	7/1	1990.05.05	7	237	4	+1
44	Mignano Monte Lungo (CE)	41.404	13.983	+	8/1	1980.11.23	9.5	132	7	+1
45	Mineo (CT)	37.266	14.691	+/-	10/2	1905.09.08 1980.01.23	11 5.5	186 43	5 2	+3 -1
46	Mirabella Elcano (AV)	41.042	14.996	+	13/1	1980.11.23	9.5	33	8	+1
47	Moio Alcantara (ME)	37.899	15.051	-	11/3	1905.09.08 1908.12.28 1975.01.16	11 11 7	117 57 53	3 5 1	-1 -1 -1
48	Mongrassano (CS)	39.526	16.111	-	7/1	1908.12.28	11	152	5	-1
49	Montalto Uffugo (CS)	39.405	16.158	+	9/1	1990.05.05	7	174	5.5	+1.5
50	Monte Castello di Vibio (PG)	42.840	12.352	-	8/2	1993.06.05 1997.09.26	6 9	39 45	1 4	-1 -1
51	Monteleone, (VV) Vibo Valentia	38.675	16.102	-	10/1	1638.03.27	11	45	6.5	-1
52	Montemurro (PZ)	40.297	15.991	+	10/2	1905.09.08 1980.11.23	11 9.5	181 95	6 7	+1 +1
53	Montevarchi (AR)	43.523	11.568	+	18/1	1915.01.13	11	246	6	+2
54	Narni (TR)	42.517	12.521	+	19/1	1998.08.15	6	47	4	+1
55	Nocera Inferiore (SA)	40.743	14.642	+	15/1	1991.05.26	6.5	100	4.5	+1
56	Nola (NA)	40.926	14.529	-	12/2	1688.06.05 1991.05.26	11 6.5	37 117	5 1	-1 -1.5
57	Notaresco (TE)	42.657	13.894	+	9/1	1984.05.07	8	112	6	+2
58	Nusco (AV)	40.887	15.085	-	8/1	1930.07.23	10	25	5	-1
59	Osimo (AN)	43.485	13.483	+	22/1	1741.04.24	9	39	8	+1
60	Parma (PR)	44.801	10.329	+	25/1	1989.10.03	4	35	3	+2
61	Paternò (CT)	37.566	14.902	+	13/1	1905.09.08	11	151	6	+1
62	Pienza (SI)	43.079	11.679	+	8/1	1993.06.05	6	81	3	+2
63	Pizzoli (AQ)	42.435	13.303	+	11/1	1933.09.26	9	78	7	+1
64	Porcia (PN)	45.964	12.618	+	10/1	1976.05.06	9.5	46	8	+1

#	Site g_0 (province)	coordinates		type $s(g_0)$	$f(g)=$ N_{map}/N_a	I -map ^{*)}				
		Lat	Long			EQ date	I_0	dist	$I(g_0)$	$\Delta I(g_0)$
65	Porretta (BO)	44.156	10.976	-	12/2	1909.01.13	6.5	74	3	-1
						1920.09.07	9.5	60	4	-1
66	Portomaggiore (FE)	44.697	11.805	+	13/1	1916.05.17	7.5	105	6	+1
67	Prato (PO)	43.879	11.096	+	22/1	1983.11.09	6.5	123	5	+1
68	Quero (BL)	45.921	11.931	-	7/1	1895.04.14	8.5	169	4	-1
69	Raccuja (ME)	38.055	14.901	+	7/1	1905.09.08	11	115	7	+1
70	Rapolla (PZ)	40.976	15.675	+	7/2	1990.05.05	7	37	7	+1
						1991.05.26	6.5	41	6.5	+1
71	Rignano Garganico (FG)	41.675	15.587	-	8/1	1962.08.21	9	69	4	-2
72	Rocca di Papa (RM)	41.760	12.710	+	12/2	1898.06.27	7.5	71	5	+1
						1995.06.12	5.5	24	5	+1
73	Rocca San Casciano (FC)	44.060	11.842	-	17/1	1920.09.07	9.5	131	1	-2
74	Rosarno (RC)	38.487	15.978	+	9/1	1894.11.16	8.5	23	8	+1
75	Rovigo (RO)	45.070	11.790	+	15/1	1983.11.09	6.5	114	5	+1
76	San Marco la Catola (FG)	41.525	15.006	+	9/1	1995.09.30	6	52	5.5	+1
77	San Martino Sannita (BN)	41.066	14.837	+	7/2	1805.07.26	10	60	8	+1
						1990.05.05	7	61	6.5	+1
78	San Paolo di Civitate (FG)	41.739	15.261	-	8/1	1980.11.23	9.5	101	4	-1
79	San Pio delle Camere (AQ)	42.286	13.656	+	7/1	1990.05.05	7	242	4	+1
80	San Severino Marche (MC)	43.229	13.177	+/-	18/4	1972.11.26	7.5	44	4	-1
						1980.11.23	9.5	341	5	+1
						1987.07.03	7	40	6	+1
						1993.06.05	6	39	2	-1
81	Sassoferrato (AN)	43.434	12.858	-	22/1	1984.04.29	7	32	4	-1
82	Sellano (PG)	42.888	12.926	+	20/1	1987.07.03	7	59	5	+1
83	Staffolo (AN)	43.432	13.186	+/-	12/2	1741.04.24	9	18	5.5	-1
						1979.09.19	8	78	6	+1
84	Stornarella (FG)	41.256	15.731	-	8/2	1913.10.04	7.5	96	1	-1.5
						1991.05.26	6.5	71	3	-1
85	Subiaco (RM)	41.925	13.095	+	19/1	1979.09.19	8	91	6	+1
86	Sulmona (AQ)	42.047	13.928	+	23/2	1933.09.26	9	18	8	+1
						1987.07.03	7	127	6	+2
87	Toro (CB)	41.570	14.766	+	7/1	1990.05.05	7	114	4.5	+1
88	Torrecuso (BN)	41.189	14.679	+/-	10/2	1991.05.26	6.5	121	5	+2
						1990.05.05	7	82	1	-3
89	Trivigno (PZ)	40.580	15.990	+	10/1	1905.09.08	11	213	6	+1
90	Urbino (PU)	43.726	12.636	+	35/4	1873.03.12	7.5	78	6.5	+1
						1904.11.17	7	122	3	+2
						1907.01.23	5.5	154	3.5	+2
						1915.01.13	11	212	6	+1
91	Vacone (RI)	42.384	12.644	-	8/1	1979.09.19	8	47	4	-1
92	Vallata (AV)	41.034	15.253	+	8/1	1991.05.26	6.5	69	5.5	+1
93	Vallombrosa (FI)	43.731	11.588	+	10/1	1914.10.27	7	94	6	+1
94	Velletri (RM)	41.688	12.778	+	13/1	1990.05.05	7	255	3.5	+1.5
95	Venafro (IS)	41.485	14.044	+	15/2	1997.03.19	6	65	3	+2
						1990.05.05	7	149	6.5	+1.5
96	Vicenza (VI)	45.549	11.549	+	14/1	1983.11.09	6.5	119	5	+1

*) EQ, earthquake; I_0 , intensity at epicenter; dist, distance from g_0 in km.